46th International SAMPE Symposium
May 6–10, 2001

THE STUDY OF EMPIRICAL METHODOLOGY TO OBSERVE DAMPING CHARACTERISTICS OF VARIOUS LAMINATE COMPOSITE PLATES

Faysal Kolkailah, Elthary Elghandour,
Taikha Oh, and Jason Bolosan
Department of Aerospace Engineering,
California Polytechnic State University,
San Luis Obispo, California, USA.

ABSTRACT

Modifying the stiffness of the structure is usually not a feasible solution to enhancing damping, since changing the stiffness effects the natural frequency changing and eventually the condition of resonance will be reached. Therefore, one of the recommendatory ways to reduce the response on structural elements is to improve damping characteristics. The objectives of this study are to present empirical methodology to detect damping characteristics of structural elements, and determine the optimal location of sensor to detect structural failure by analyzed data from both experimental and numerical analysis. Using orthotropic composite plates comprised of 977-2 Carbon fiber/IM7 epoxy, the natural frequencies of structural bending modes and damping ratio of the composite plates were experimented by free vibration test, and then comparison was made between the experimental results and the numerical analysis done by finite element method. The effectiveness of crack on a structure in damped free vibration was confirmed by the analysis using edge-notched composite plate. The results represented the natural frequency of a composite plate was consistent with changing sensor location, and showed good agreement for both experimental and numerical analysis.

KEY WORDS: Composite Structures, Carbon Fiber, Application-Aerospace

1. INTRODUCTION

A large number of investigations on the structural dynamic response of plates subjected to acoustic loads and the problem of determining crack position via dynamic characterization of the structure exist in the literature. Cawley and Adams[4] were the first researchers who proposed the theorem of that the ratio of two natural frequency changes is a function only of the crack position. As a consequence, the crack sizing and location tasks for a single cracked beam are relatively straightforward in that it would be possible to address independently the tasks of quantification and localization. Seide and Adami[5] studied a large deflection of a buckled beam in random response, and Lee[8] studied isotropic rectangular plates with either simply supported or clamped edges. Stubbs and Osegueda[6-7] presented a method for structural damage identification that relates changes in the natural frequencies to changes in member stiffness with a sensitivity relation. Moreover, they demonstrated that this sensitivity method becomes difficult when the number of modes is much fewer than the number of damage parameters. Hu and Liang[8] proposed a two-step procedure to identify cracks in beam structures. They used the effective stress concept coupled with Hamilton's principle to derive a formulation equivalent to the Stubbs and Osegueda[6-7] sensitivity equations. By using this formulation the elements of the structure that contain cracks could be identified, and then a spring damage model was used to quantify the location and depth of the crack in each damaged element. The Galerkin' equivalent linearization method[6] and Newmark's theorem for a random response were developed to obtain the numerical simulation of time domain response. More recently, Venkatesh et al[12] applied the Galerkin's numerical simulation[5] approach to simply supported metal and orthotropic composite rectangular plates. Kolkailah and Elghandour[1-2] developed preliminary methodology of the sensor/actuator optimizing for damped random vibration using surface mounted piezoelectric sensors in 1997.

2. EXPERIMENTAL PROCEDURES

All composite plates have 8 in. x 4 in. x 0.5 in. geometric dimension and the dimension of aluminum 2024 plate is 8 in. x 4 in. x 0.635 inches. The composite

plates were comprised of eight layers of 977-2 Carbon fiber/IM7 epoxy and each layer was symmetric cross-plied by an orientation in $[0/0/90/90]_s$, $[90/0/90/0]_s$, and $[90/90/0/0]_s$. Since each lamina of the composite plate is an unidirectional lamina, the lamina is an orthotropic material with principal material axis in the direction of the fiber (longitudinal), normal to the fibers in the plane of lamina (in-plane transverse), and normal to the plane of the lamina. Table 1 shows the material properties of 977-2 Carbon fiber/IM7 epoxy in manufactur-ing stage.

TABLE 1. MATERIAL PROPERTIES FOR 977-2 CARBON FIBER/IM7 EPOXY

Material Properties	Symbol	Value	Units
Elastic modulus in 0°	E_L	2.5e7	psi
Elastic modulus in 90°	E_T	1.1e6	psi
Density	ρ	3.98e-4	$lb*s^2/in^4$
Poisson's Ratio	ν	0.36	N/A

The composite plates were fabricated by using a Composite Air Press machine. Before any pressing occurred the air press was carefully cleaned to remove any old debris, which could lead to deformation in the finished plate. The Air Press was used for the curing cycle of the laminated plates and is programmable for four different time and temperature curing cycles consists of two heating and one cooling step. The curing cycle for the composite plates begins with an initial temperature of 75°F and gradually increases to 250°F for 58 minutes. The temperature is then held constant for two hours before increasing to 350°F in 33 minutes. After three hours and 33 minutes, the temperature is decreased to 75°F within a period of 90 minutes and is maintained at this temperature for five minutes before completing the cycle. The entire curing cycle is over nine and a half hours long. After fabricating plates was done, each plate was tested using electromagnetic shaker (Figure 1) to determine the locations of piezoelectric sensors based on structural bending mode shape. In order to pinpoint the first three

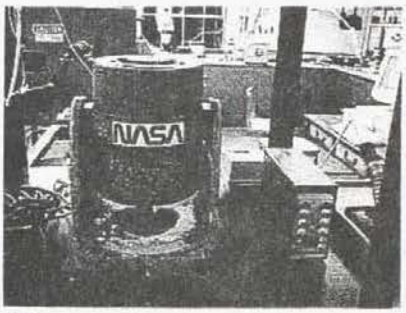

Figure 1 : Electromagnetic shaker

structural bending modes, small amount of sugar granules were poured on the plate. When the sugar granules formed straight lines, the locations of ***zero displacement*** on the plate could be detected. The grains of sugar formed one, two and three distinct lines on the plates representing the node of the first, second, and third bending mode, respectively. By counting the number of locations with zero displacement, the piezoelectric sensors were placed on the plates where the locations of the structural bending modes were discovered. Small prototype parts were cut from piezoceramic sheet stock by using a razor blade and a straight edge to score the piezo surface and then making a controlled break. Four pieces of piezoelectric sensors, using electronic conductive adhesive (cyanoacrylate), were bonded on a plate, then one electrical lead was attached to the substrate, and one to the outward face of the piezoceramic sheet. In order to convenience, each of composite plates was named by its stacking orientation as follows;

Composite Plate I : $[90/90/0/0]_s$
Composite Plate II : $[0/90/0/90]_s$
Composite Plate III : $[0/0/90/90]_s$

The composite plate with edge notches was fabricated as same procedure, and then the location of crack and sensor was decided by the results of finite element model simulation. The simulation results represented the consistency of frequency response about the different sensor locations and stacking structures, thus it would flexible to select a specimen among the different plates. The effects of the size of cracks were also simulated in the length of 0.1 – 1 inch. Based on the finite element analysis results, two 0.5 inches edge notches were placed at 0.35 inches from the left hand corner on composite plate II, and a piezoelectric sensor mounted at the center of plate near the location of crack. Figure 2 shows the pictures of specimen plates with wiring piezoelectric sensors.

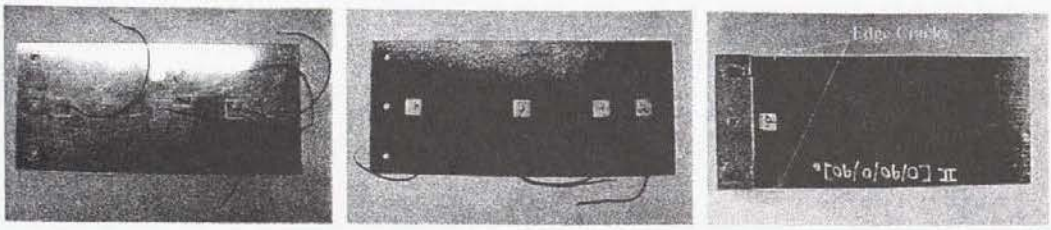

Figure 2 : Specimen plates
(Left: aluminum 2024, Middle: un-cracked composite, Right: edge-notched composite)

3. RESULTS AND DISCUSSIONS

3.1 Experimental results for un-cracked plates The chirp signal is used to model optical diffraction as convolution with a constant-magnitude complex quadratic phase signal. The quadratic-phase signal is a generalization of the sinusoid where the oscillation frequency varies linearly with coordinate. Figure 3 shows the frequency response functions for different composite plates excited by chirp input signal. In the FRF plot, each overshoot corresponds to a resonance frequency of a plate in a certain structural bending mode. The green line shows frequency response of composite plate I, red line corresponds to composite plate II, brown and blue lines show frequency response of composite plate III and aluminum 2024 plate, respectively. Reading numeric values at the peaks form the FRF visually identified the fundamental resonance frequencies for each bending mode, and these values were compared to the values obtained by numerical analysis using FEM. For all composite plates, the first group of peaks under the bandwidth of 100 Hz corresponds to the natural frequency response of first bending mode, and the frequency values match numerical analysis values done by using finite element models within 1 - 5% error tolerance. This error would be attributed to experimental error or signal noise in the function generator. The resonance frequencies of second bending mode were varied in a range of 160 – 380 Hz depended on a plate. However, it was difficult to detect the resonance frequency of composite plate II and III in higher structural modes with sensor #4. The difficulty caused the location of sensor #4 was relatively far from the source of excitation (in this case, the cramped point near sensor location #1), and the strain around sensor #4 due to the vibration was relatively smaller than other sensor locations, hence the response of sensor #4 was not amplified with high fidelity.

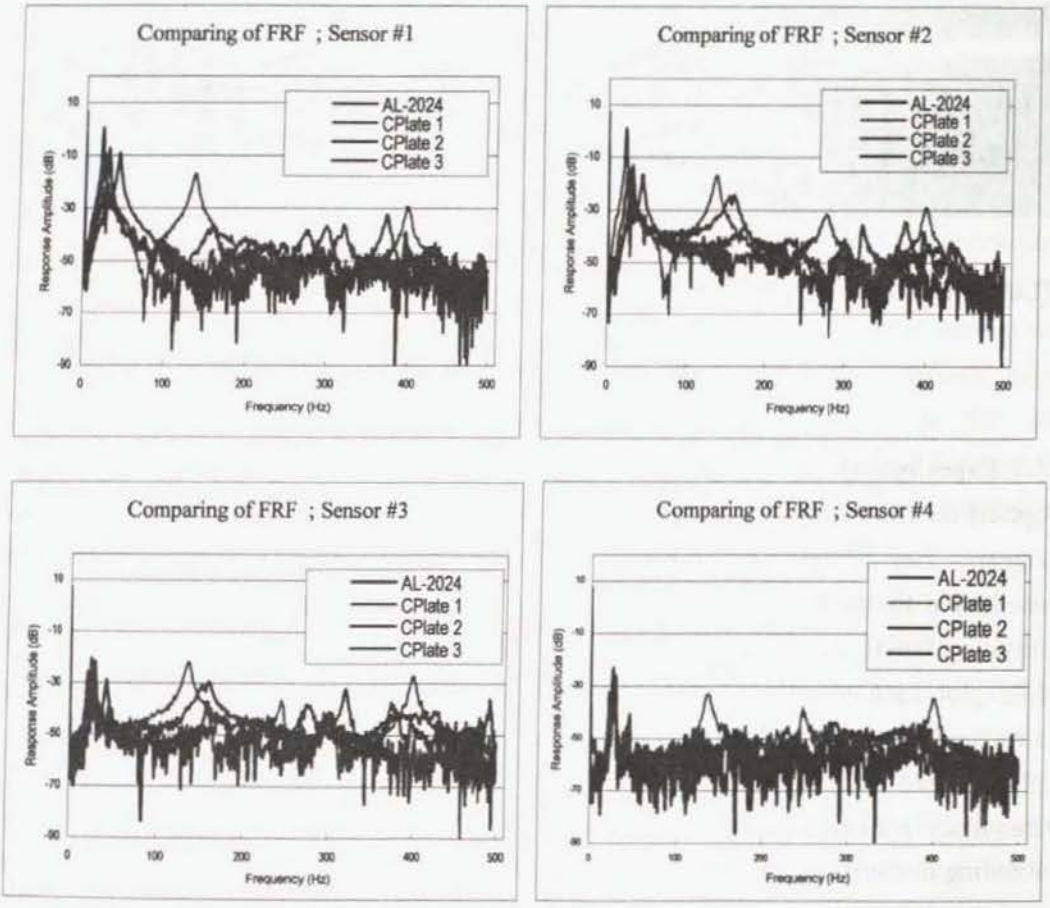

Figure 3 : Frequency response function for different plates by chirp excitation

For the all sensors on the plates, the resonance frequencies of the first structural bending mode were consistent, and detected with high accuracy. However, the sensor #3 and #4, which located relatively far from the source of excitation, showed difficulty to detect the accurate frequencies of higher bending modes. Composite plate I and aluminum 2024 plate responded with higher magnitudes of response amplitude, and sensor #1 and #2 mostly detected the change of response amplitude accurately. Recalling from the figure 3, it was significant that the different structural elements were effective on the natural frequency of the each bending mode, e.g., the first bending mode was effected by changing stacking orientation of composite laminar and material, and the second bending mode was more effected by changing

structure. These results provided a standpoint to determine the location of sensors on the structure in a motion subjected to low frequency and high impedance, and it would be applicable to the sensor optimizing of crack detection. Table 2 shows the numeric value ranges of resonance frequency and amplitude of each plate at different bending modes obtained from experiments, and Table 3 represents the predicted resonance frequencies of each plate for three different bending modes obtained by finite element modal simulation.

TABLE 2. EXPERIMENTAL MODAL FREQUENCIES

	Mode 1	**Mode 2**	**Unit**
CPlate I	21 - 22	131 -139	Hz
CPlate II	**25 - 31**	**298 -310**	**Hz**
CPlate III	42 - 44	375 - 382	Hz
AL -2024	**24 - 26**	**161 - 167**	**Hz**

TABLE 3. PREDICTED MODAL FREQUENCIES

	Mode 1	Mode 2	Unit
CPlate I	21.39	131.86	Hz
CPlate II	26.14	272.97	Hz
CPlate III	48.86	305.73	Hz
AL -2024	26.77	166.52	Hz

3.2 Experimental results for cracked plates The composite plate with edge notches was tested as same procedure with un-cracked plates, but additional sinusoidal excitation tests conducted to investigate damping ratio (ζ) using by logarithmic decrement method. Figure 4 represents the frequency response functions (FRF) and time history plots for cracked plate comparing to the response on un-cracked plate.

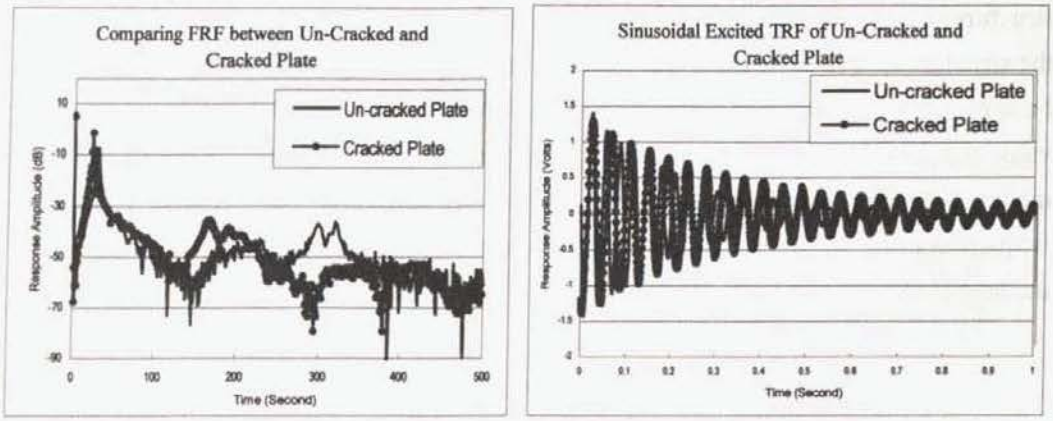

Figure 4 : Comparing frequency response function and time history for both un-cracked and cracked plate

The blue line shows frequency response of un-cracked plate, and red dotted line corresponds to cracked plate, respectively. Reading numeric values at the peaks form the FRF visually identified the fundamental resonance frequencies for each bending modes, and these values were compared to the values obtained by numerical analysis using FEM. As shown in the figure, the natural frequencies of the first mode for both of cracked and un-cracked plate were up to 30 Hz, and the second mode natural frequencies were approximately 200 Hz for cracked plate and 300 Hz for un-cracked plate. These frequency values were agreeable with the values of numerical analysis done by finite element model within 1 - 3% error tolerance. The comparing modal frequencies and amplitudes for un-cracked and cracked plates by experiment were provided in Table 4, and numerically predicted values were also compared. For cracked plate, the critical damping ratio was $\zeta = 0.0238$, and 2% settling time of the first mode was in less than 0.1 second. The critical damping ratio for un-cracked plate was a bit higher as $\zeta = 0.0278$, and 2% settling time of the first mode was in less than 0.05 second. Considering the envelope curve of time response, linear decaying of motion, about every half cycle of period, was detected for both plates. Response amplitude of cracked plate by sinusoidal excitation was also higher than that of un-cracked plate as shown in chirp excitation.

TABLE 4. COMPARING MODAL FREQUENCIES

	Mode 1	Mode 2	Unit
Un-Cracked Plate (Experiment)	30.29	298.86	Hz
Un-Cracked Plate (Numerical)	26.14	272.97	Hz
Cracked Plate (Experiment)	23.44	169.02	Hz
Cracked Plate (Numerical)	25.67	165.88	Hz

From the sinusoidal excitation tests, the damping ratio of each plate calculated from the logarithmic decrement of the time response is organized in Table 5.

TABLE 5. DAMPING RATIO

Plate	Damping ratio (ζ)
Un-cracked plate	0.0278
Cracked plate	0.0238

4. CONCLUSIONS

The resonance frequencies of structural bending mode for various laminated composite plates have been consistent about the notch and sensor locations. The simulation of finite element model to analyze the dynamics characteristics of laminated composite plate with cracks has made reasonable agreement to the experimental vibration data. Composite plate I and aluminum 2024 plate responded with higher magnitudes of response amplitude, and the sensors near the origin of excitation mostly detected the change of response amplitude accurately. However, the sensors, which located relatively far from the source of excitation, showed difficulty to detect the accurate frequencies of higher bending modes because the two sensors located right hand side were aligned to the second and third zero displacement lines. In the enhanced

damping system design, such as feedback system or intelligent structural design, the constitutive relationships - laminar stacking sequence, sensor location, and material properties - would be necessarily considered to obtain mode shape and frequency from the finite element formulation. It might be challenging to generalize the sensor location for random shaped cracks in high order frequency response modes and structural bending modes in future works.

5. REFERENCES

1. Kolkailah, Faysal A. and Elghandour, E., Optimizing Piezoelectric Sensors /Actuators for Vibration Damping, NASA Joint Research Interchange #NCAA2-779, California Polytechnic State University, (1993).
2. Kolkailah, Faysal A. and Elghandour, Eltahry, Hybrid Damping System for an Electronic Equipment Mounting Shelf, California Polytechnic State University, San Luis Obispo, Interchange No. NCC2-5110, (1997).
3. Cawley, P. and Adams, A., The location of defects in structures from measurements of natural frequencies, Journal Strain Analysis for Engineering Design, 1979, pp. 49-57.
4. Seide, P. and Adami, C., Dynamic Stability of Beams in a Combined Thermal-Acoustic Environment, AFFWAL-TR-83-3027, Wright-Patterson, (1983).
5. Stubbs, N. and Osegueda, R., Global non-destructive damage evaluation in solids, International Journal of Analytical and Experimental Modal Analysis, pp. 67-79, (1990).
6. Stubbs, N. and Osegueda, R., Global non-destructive damage evaluation in solids - experimental verification, International Journal of Analytical and Experimental Modal Analysis, 1990, pp. 81-97.
7. Hu, J. and Liang, Y., An integrated approach to detection of cracks using vibration characteristics, Journal of the Franklin Institute, 1993, pp. 841-853.
8. Wang, A. and Ertepinar, A., Large Amplitude Oscillations of Laminated Thick-Walled Spherical Shells Using Galerkin's Method, in Computer Aided Engineering, Vol. 5 - Advances in Solid Mechanics, University of Waterloo, 1971, pp. 603-614.

9. Boucher D., Langier M., and Maerfeld C., Computation of the vibrational modes for piezoelectric array transducers using a mixed finite element-perturbation method, IEEE Trans. Sonics Ultrason., SU-28, 1981, pp. 318-330.
10. Lee, J., Large-Amplitude Plate Vibration in an Elevated Thermal Environment, WL-TR-92-3049, Wright-Patterson AFB, (1992).
11. Schulz, M. J., Abdelnaser, A. S., Pai, P. F., Linville, M. S., and Chung, J., Detecting Structural Damage Using Transmittance Functions, International Modal Analysis Conference, Orlando, Florida, (1997).
12. Venkatesh, A., Hilborn, J., Bidaux, J. E. and Gotthardt, R., Active Vibration Control of Flexible Linkage Mechanisms Using Shape Memory Alloy Fiber-Reinforced composites, The 1st European Conference on Smart Structures and Materials, Glasgow, UK, 1992, pp. 185 - 188.